 DOI 10.1002/mnfr.201000528 *Mol. Nutr. Food Res.* 2011, *55*, 1096–1103

RESEARCH ARTICLE

Fabrication of nanoparticles using partially purified pomegranate ellagitannins and gelatin and their apoptotic effects

Zheng Li, Susan S. Percival, Suzanna Bonard and Liwei Gu

Department of Food Science and Human Nutrition, Institute of Food and Agricultural Sciences, University of Florida, Gainesville, FL, USA

Received: October 20, 2010
Revised: December 1, 2010
Accepted: December 16, 2010

Scope: Nanoparticles possess unique chemical and biological properties compared to bulk materials. Bioactive food components encapsulated in nanoparticles may have increased bioavailability and bioactivities.

Methods and results: Self-assembled nanoparticles made of partially purified pomegranate ellagitannins (PPE) and gelatin were fabricated using three PPE-to-gelatin mass ratios (1:5, 5:5, and 7:5). The PPE contained 16.6% (w/w) of punicalagin A, 32.5% (w/w) of punicalagin B, and a small amount of ellagic acid-hexoside and ellagic acid (1%, w/w). Nanoparticles fabricated using the ratio 5:5 had a particle size of 149.3 ± 1.8 nm, positive zeta-potential of 17.8 ± 0.9 mV, production efficiency 53.0 ± 4.2%, and spherical morphology under scanning electron microscopy. Loading efficiency of punicalagin A and punicalagin B in these particles were 94.2 ± 0.4% and 83.8 ± 0.5 %, respectively. Loading capacity was 14.8 ± 1.5% and 25.7 ± 2.2%, respectively. Only punicalagin anomers were able to bind with gelatin to form nanoparticles, whereas ellagic acid-hexoside or ellagic acid could not. Fourier transform infrared spectroscopy suggested that the interactions between ellagitannins and gelatin were hydrogen bonding and hydrophobic interactions. PPE-gelatin nanoparticle suspension was less effective than PPE in inducing the early stage of apoptosis on human promyelocytic leukemia cells HL-60. But they had similar effects in inducing late stage of apoptosis and necrosis.

Conclusion: Pomegranate ellagitannins bind with gelatin to form self-assembled nanoparticles. Ellagitannins encapsulated in nanoparticles had decreased apoptotic effects on leukemia cells HL-60.

Keywords:
Ellagitannin / Gelatin A / Nanoparticle / Pomegranate / Punicalagin

1 Introduction

Nanoparticles are defined in biological sciences as particles with at least one dimension less than 1000 nm [1]. They possess many unique chemical, biological, and physical properties compared to bulk materials. Drugs or other bioactive ingredients encapsulated in nanoparticles or other nanocarriers had drastically increased bioavailability and bioactivity. For instance, epigallocathecin gallate (EGCG) encapsulated in nanoparticles was 10-fold as effective as EGCG that was not encapsulated [2]. Carboplatin-loaded chitosan-alginate nanoparticles showed greater antiproliferative activities and apoptotic effects compared to the drug in solution [3]. Cisplatin-incorporated in gelatin nanoparticles provided stronger antitumor activities and was less toxic compared to free cisplatin in vivo [4].

Pomegranate contains several types of ellagitannins, including punicalagin, punicalin, gallagic acid, ellagic acid, and ellagic acid-glycosides [5, 6]. These ellagitannins have been reported to prevent cancer and cardiovascular diseases,

Correspondence: Dr. Liwei Gu, Department of Food Science and Human Nutrition, Institute of Food and Agricultural Sciences, University of Florida, Gainesville, FL 32611, USA
E-mail: LGu@ufl.edu
Fax: +1-352-392-9467

Abbreviations: DLS, dynamic light scattering; **FTIR,** Fourier transform infrared; **PPE,** purified pomegranate ellagitannins; **SEM,** scanning electron microscopy

scavenge oxidative free radicals, and reduce the risk for atherosclerosis and other chronic diseases [7–10]. The affinity between tannins and proteins is a well-known phenomenon [11, 12]. The present study takes advantage of such affinity to fabricate the self-assembled nanoparticles using partially purified pomegranate ellagitannins (PPE) and gelatin. The PPE-gelatin nanoparticles, to our knowledge, have not been reported before. Three different mass ratios of PPE and gelatin were applied and characteristics of nanoparticles including particle size, zeta-potential, morphology, and interaction binding modes were measured by Microtrac Nanotrac, ZetaPlus, Scanning Electron Microscopy (SEM), and Fourier transform infrared (FTIR) spectroscopy, respectively. Loading efficiency and loading capacity of ellagitannins in the resultant nanoparticles were investigated using HPLC-ESI-MS^n. The Annexin V Staining Assay on a leukemic cell line HL-60 was selected to evaluate the apoptotic effect of PPE-gelatin nanoparticles and compare that to the PPE solution.

2 Materials and methods

2.1 Samples and chemicals

Pomegranates (*Punica granatum* L.) were obtained from Publix Supermarket (Gainesville, FL, USA). The pericarp of the fruits was manually separated. Pure punicalagin and ellagic acid was purchased from Quality Phytochemicals LLC (Edison, NJ, USA) and Sigma-Aldrich (St. Louis, MO, USA), respectively. Ethanol, formic acid, methanol, gelatin type A, and other chemicals were products of Fisher Scientific (Pittsburg, PA, USA). Amberlite XAD-16N resin was purchased from Dow Company (Piscataway, NJ, USA).

2.2 Extraction and purification of pomegranate ellagitannins

Extraction and purification of pomegranate ellagitannins followed a published method with minor modifications [6]. Frozen pomegranate pericarp (50 g) was blended in a kitchen blender and mixed with water (250 mL). The water suspension was sonicated for 5 min and kept at 25°C for 30 min. The sonication step was repeated for two more times. Water extract was obtained after filtration and then dried on an ISS110 SpeedVac evaporator (Fisher Scientific) at 25°C. The resultant solid was re-dissolved in 20 mL of water and loaded onto a column (30 × 400 mm, id × length) packed with Amberlite XAD-16N resin. The column was eluted with 2 L of water. Ellagitannins were recovered from the column using 400 mL of ethanol. Ethanol elute was evaporated at 25°C to yield PPE as dry power (approximately 2.5 g).

2.3 HPLC – ESI – MS^n analyses

An Agilent 1200 HPLC system consisting of an autosampler, a binary pump, a column compartment, a diode array detector (Agilent Technologies, Palo Alto, CA, USA) was interfaced to a HCT ion trap mass spectrometer (Bruker Daltonics, Billerica, MA, USA). PPE solution was filtered through 0.45-μm filter units and 30 μL was injected on an Agilent Zorbax ODS column (4.6 mm × 25 cm, 5 μm particle size) for separation of ellagitannins. The binary mobile phase consisted of (A) formic acid:water (2:98 v/v) and (B) formic acid:methanol (2:98 v/v). Gradient reported by Seeram et al. was used with minor modifications [6]. The gradient is described as follows: 0–30 min, 1–20% B linear; 30–45 min, 20–40% B; 45–60 min, 40–95% B; 60–65 min, 95–1% B; followed by 5 min of re-equilibration of the column before the next run. The detection wavelength on diode array detector was 378 nm. Electrospray ionization in negative mode was performed using nebulizer 65 psi, dry gas 11 L/min, drying temperature 350°C, and capillary 4000 V. The full scan mass spectra were measured at m/z 100–2000. Auto MS^2 was conducted with 50% compound stability and 60% trap drive level. Punicalagin A, B, and ellagic acid were used as external standard for quantification. Data were collected and calculated using Chemstation software (Version B. 01.03, Agilent Technologies).

2.4 Self-assembly of PPE-gelatin nanoparticles

Gelatin type A (0.5 g) and PPE powder (0.5 g) were dissolved in DI water (1000 mL) to a concentration of 0.5 mg/mL, respectively. PPE solution with 1, 5, or 7 mL was mixed with 5 mL of gelatin solution, which gave PPE-to-gelatin mass ratios of 1:5, 5:5, and 7:5, respectively. The mixture was incubated at 25°C for 48 h. The nanoparticle suspensions were then centrifuged at 12 000 rpm for 5 min. The supernatant was removed from the suspension for calculations of loading efficiency and loading capacity. The sediments were lyophilized for 48 h to form dry particles and stored at −20°C for further analyses.

2.5 Particle size and zeta-potential measurement

Mean particle size and size distribution of was measured using dynamic light scattering (DLS) on a Nanotrac ULTRA with an external probe (Microtrac, Largo, FL, USA). Each sample was analyzed in triplicate and each replicate was measured six times to yield the average particle size. Zeta-potentials were determined using Brookhaven ZetaPlus (Brookhaven Instrument, Holtsville, NY, USA). Triplicate tests were conducted at a constant temperature of 22°C and each replicate was measured ten times to obtain the average zeta-potential.

2.6 SEM

Dry particle powders were used for morphology characterization using Field Emission Scanning Electron Microscope (Model JSM-633OF, JEOL, Tokyo, Japan).

2.7 FTIR spectroscopy

PPE-gelatin nanoparticles were fabricated at a PPE-to-gelatin mass ratio of 5:5. Supernatant and nanoparticles were separated by centrifuge and freeze-dried. Dry PPE, gelatin, PPE-gelatin nanoparticles, and dried supernatant were mixed with pure KBr powders using a ratio of 1:100 sample: KBr (w/w). These mixtures were ground into fine powders and then analyzed using a Thermo Nicolet Magna 760 FTIR (Thermo Nicolet, Madison, WI, USA) with a MCT-A detector. Pure KBr powders were used as background. The FTIR spectra were obtained over the wave number range from 700 to 4000 cm^{-1} at a resolution of 2 cm^{-1}.

2.8 Production efficiency, loading efficiency, and loading capacity measurements

Production efficiency was defined as (weight of dry particles)/(total weight of PPE and gelatin used for fabrication). Supernatant from the nanoparticle suspension was filtrated through 0.45-μm filter units and injection volume of 30 μL was injected for HPLC-ESI-MS^n. The loading efficiency was defined as (ellagitannin used for fabrication-ellagitannin in supernatant)/(ellagitannin used for fabrication). The loading capacity was defined as (weight of ellagitannin embedded into nanoparticles)/(weight of dry nanoparticles).

2.9 Cell apoptosis

Annexin V staining was used for cell apoptosis measurements in the HL-60 cell line. Four PPE-gelatin nanoparticle suspension samples were prepared, and each PPE-gelatin nanoparticle suspension with the concentrations of 0.0156, 0.0313, 0.0625, and 0.125 mg/mL was added to the appropriate wells in triplicates. PPE solutions with the concentrations of 0.0156, 0.0313, 0.0625, and 0.125 mg/mL were added to wells in triplicates. HL-60 cells in IMDM media (100 μL containing 120 000 cells) were seeded into each well of a 48-well tissue culture plate (Costar, Corning, NY, USA). Four hundred microliter of IMDM (Lonza, Basel, Switzerland) complete media (100 000 U/L penicillin; 100 mg/L streptomycin; 0.25 mg/L fungizone; 50 mg/L gentamicin) was added. The plate was incubated for 22 h at 37°C in a 7.5% CO_2 humidified atmosphere. Cell apoptosis was measured by following the Annexin V staining protocol (eBioscience, San Diego, CA, USA). At 22 h, the HL-60 cells were harvested and washed once in PBS and diluted binding buffer, respectively. Then, cells were re-suspended in diluted binding buffer (100 μL) and fluorochrome-conjugated Annexin V was added and incubated for 15 min at room temperature. Cells were washed again in diluted binding buffer and resuspended in 200 μL of diluted binding buffer. Propidium iodide in PBS (5 μL) was added to cells and the cells were then analyzed on a 3-color fluorescence FACsort Flow Cytometer (Becton Dickinson, San Jose, CA, USA) at the UF ICBR Flow Cytometry core facility within 2 h. Data were analyzed with FlowJo software (TreeStar, version 7.6).

2.10 Data analyses

Data were expressed as mean ± standard deviation. One-way analyses of variance with Tukey-HSD comparison of the means were performed using JMP software (Version 8.0, SAS Institute, Cary, NC, USA). Student's *t*-test was use to compare data from two independent groups. A difference with $p \leq 0.05$ was considered significant.

3 Results

3.1 Ellagitannin identification and quatification

The PPE were extracted and partially purified using porous adsorption resin. Chromatogram of PPE showed four peaks that corresponded to four ellagitannins (Fig. 1). Peak identification (Fig. 2) was based on mass and product ion spectra [6]. Peaks **1** and **2** were identified as punicalagin anomer A and B according to $[M\text{-}H]^-$ m/z 1083 and a product ion at m/z 781, which suggested the existence of punicalin and ellagic acid moiety. Peak **3** had a deprotonated ion at m/z 463 and a product ion at m/z 301 formed by ellagic acid. This peak was identified as ellagic acid-hexoside. Peak **4** had a deprotonated ion at m/z 301, which was identified as ellagic acid. Punicalagtin A and B were major ellagitannins in PPE, and the contents of punicalagin A and B were 166.2 ± 3.0 and 324.6 ± 0.4 mg/g, respectively. The contents of ellagic acid-hexoside and ellagic acid were 3.4 ± 0.6 and 7.5 ± 0.0 mg/g, respectively.

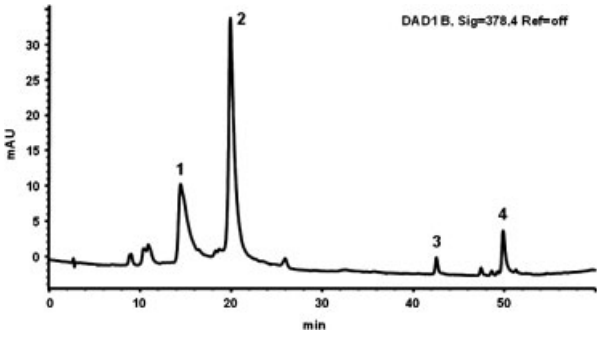

Figure 1. HPLC chromatogram of PPE solution. Peaks **1**, **2**, **3**, and **4** are punicalagin A, punicalagin B, ellagic acid-hexoside, and ellagic acid, respectively.

3.2 Characteristics of ellagitannin-gelatin nanoparticles

PPE-gelatin nanoparticles were fabricated using three different PPE-to-gelatin mass ratios (Table 1). The mean sizes of particles from the PPE-to-gelatin mass ratios at 1:5, 5:5, and 7:5, measured using DLS were 101.9 ± 9.0, 149.3 ± 1.8, and 228.5 ± 4.9 nm, respectively. The particle size increased significantly with the increase of PPE-to-gelatin mass ratio. SEM image showed that PPE-gelatin nanoparticles fabricated under these mass ratios had a spherical or approximately spherical morphology (Fig. 3). Mean zeta-potentials of these formed nanoparticles were around +18 mV, indicating that PPE-gelatin nanoparticles had a positive charge on the surface.

Interaction bindings between PPE and gelatin were assessed with FTIR spectra (Fig. 4). The FTIR spectra of gelatin (Fig. 4A) showed the typical amides I and II peaks at 1699 and 1558 cm^{-1}, respectively. The amide I absorption was mainly due to carbonyl C = O stretching vibration, whereas the amide II band consisted both C-N stretching and C-N-H in plane bending [13, 14]. Peaks at 1728 and 1599 cm^{-1} in the FTIR spectra of PPE (Fig. 4B) resulted from carbonyl stretching vibration [15, 16]. FTIR profile (Fig. 4C) of supernatant from PPE-gelatin nanoparticle suspension system was similar to that of PPE (Fig. 4B). However, FTIR spectra (Fig. 4D) of PPE-gelatin nanoparticles showed peaks at 1664 and 1535 cm^{-1}, both of which resulted from peak shifts of PPE and gelatin toward lower wavenumbers. It suggested that both amide I and II and carbonyl C = O in PPE were involved in PPE-gelatin binding and α-helical configuration was formed in PPE-gelatin nanoparticles [13, 14, 17]. The primary interaction binding forces were hydrogen-bonding and hydrophobic interactions [18].

3.3 Production efficiency, loading efficiency, and loading capacity

Among the four ellagitannins identified from the PPE, only punicalagin anomers had the capacity to bind gelatin to form PPE-gelatin nanoparticles (Table 2). Production efficiency (%) was the weight of dry nanoparticles divided by total weight of PPE and gelatin that were used. The production efficiency of nanoparticles at mass ratios 1:5, 5:5, and 7:5 were 18.5 ± 4.9, 53.0 ± 4.2, and 62.0 ± 2.8%, respectively. Loading efficiency is defined as the ratio of ellagitannins adsorbed into nanoparticles to total ellagitannins used. Loading efficiency of punicalagin A under PPE-to-gelatin mass ratios at 1:5, 5:5, and 7:5 were 57.5 ± 2.7, 94.2 ± 0.4, and 69.1 ± 4.4%, respectively. Loading efficiency of punicalagin B were 29.5 ± 0.2, 83.8 ± 0.5, and 67.2 ± 0.2%, respectively. Loading capacity (% w/w) is the content of

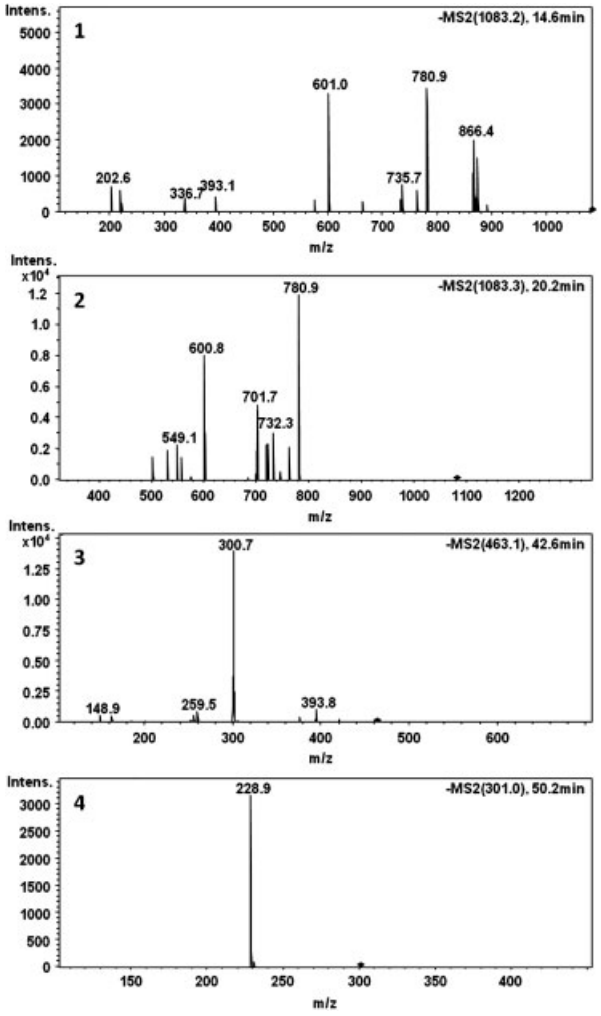

Figure 2. Product ion spectra (MS^2) of punicalagin A (**1**), punicalagin B (**2**), ellagic acid-hexoside (**3**), and ellagic acid (**4**).

Table 1. Particle size, zeta-potential, and production efficiency of nanoparticles fabricated using three PPE-to-gelatin mass ratios

Volume of PPE solution (mL)	Volume of gelatin solution (mL)	PPE-to-gelatin mass ratio	Particle size[a)] (DLS, nm)	Zeta-potential (mV)	Production efficiency (%)
1	5	1:5	101.9 ± 9.0 c[b)]	18.3 ± 1.2 a	18.5 ± 4.9 b
5	5	5:5	149.3 ± 1.8 b	17.8 ± 0.9 a	53.0 ± 4.2 a
7	5	7:5	228.5 ± 4.9 a	18.0 ± 1.3 a	62.0 ± 2.8 a

a) Data are mean ± SD ($n = 3$). Duplicate tests were done for production efficiency.
b) Means within a column followed by the same letter are not significantly different at $p \leq 0.05$.

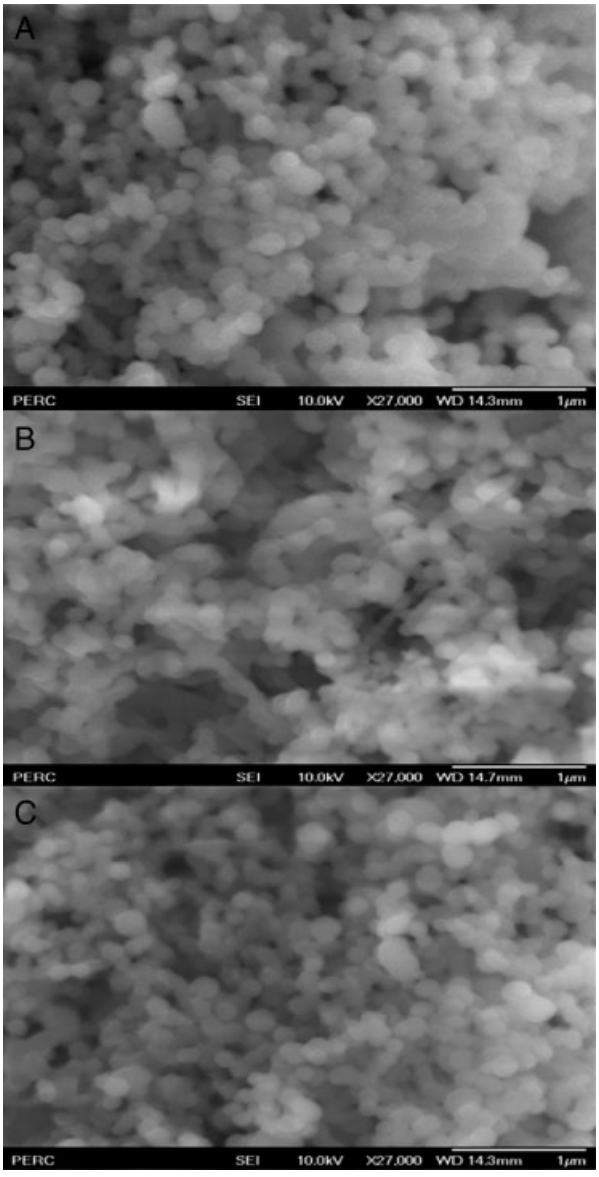

Figure 3. Morphology of PPE-gelatin nanoparticles using scanning electron microscopy (SEM) using PPE-to-gelatin mass ratios of 1:5 (A), 5:5 (B), and 7:5 (C), respectively.

ellagitannins in dry nanoparticles. Loading capacity of punicalagin A under PPE-to-gelatin mass ratios at 1:5, 5:5, and 7:5 was 9.0 ± 2.6, 14.8 ± 1.5, and $10.8 \pm 0.1\%$, respectively. Loading capacity of punicalagin B was 9.0 ± 2.4, 25.7 ± 2.2, and $20.5 \pm 0.1\%$, respectively.

3.4 Apoptosis

Apoptotic properties of pomegranate PPE-gelatin nanoparticles and PPE solution were evaluated using HL-60 cancer cell line at four concentrations. Cells that are in the early stage of apoptosis stain positive for Annexin V but negative for propidium iodide. Necrotic cells and cells at the late stage of apoptosis stain positive for both Annexin V and propidium iodide. PPE solution was more effective than PPE-gelatin nanoparticle suspension in inducing the early stage of apoptosis (Fig. 5A). The differences were not significant at the lowest concentration but became significant as the concentrations increased. At concentrations from 0.0156 to 0.0625 mg/mL, no significant differences were observed between PPE-gelatin nanoparticle suspension and PPE solution in inducing late stage of apoptosis and necrosis (Fig. 5B). However, at the higher concentration (0.125 mg/mL), PPE-gelatin nanoparticles suspension was more effective than PPE solution ($p = 0.0144$).

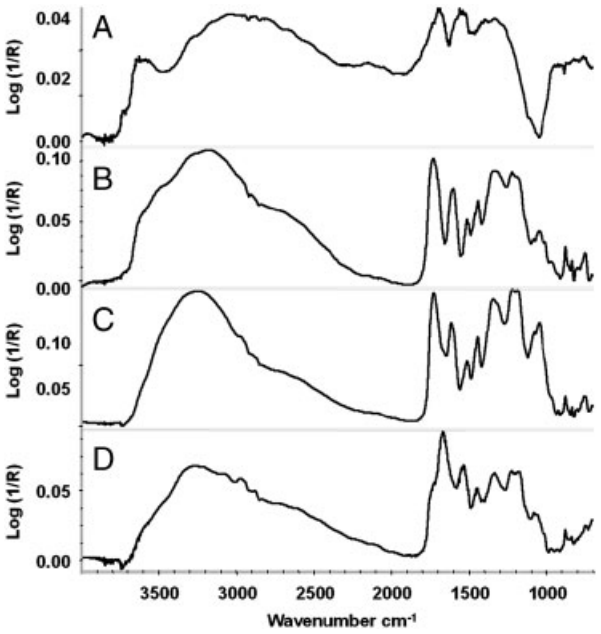

Figure 4. Fourier transform infrared (FTIR) spectra of gelatin (A), PPE (B), freeze-dried supernatant (C), and freeze-dried PPE-gelatin nanoparticles (D).

4 Discussion

PPE-gelatin nanoparticles formed spontaneously due to affinity between ellagitannins and gelatin. Gelatin has an extended random coil conformation in aqueous solution because it contains higher amounts of proline residues than other proteins or polypeptides [19]. Gelatin and tannin molecules bind to each other when they are mixed in solution [19, 20]. Magnitudes and selectivity of such binding is determined by molecular weight and tertiary structures of tannins. It has been proposed that tannins of higher molecular weight have more hydroxyl groups and hydrophobic sites, and thus enhance the interaction with gelatin [20, 21].

Table 2. Content, loading efficiency, and loading capacity of individual ellagitannin in nanoparticles fabricated using different PPE-gelatin mass ratios

Ellagitannin compound		Punicalagin A[a)]	Punicalagin B	Ellagic acid-hexoside	Ellagic acid
Content in dry PPE powder (mg/g)		166.2±3.0	324.6±0.3	3.4±0.6	7.5±0.0
Loading efficiency (%)	1:5	57.5±2.7 c	29.5±0.2 c	ND[b)]	ND
	5:5	94.2±0.4 a	83.8±0.5 a	ND	ND
	7:5	69.1±4.4 b	67.2±0.2 b	ND	ND
Loading capacity (%, w/w)	1:5	9.0±2.6 b	9.0±2.4 b	ND	ND
	5:5	14.8±1.5 a	25.7±2.2 a	ND	ND
	7:5	10.8±0.1 ab	20.5±0.1 a	ND	ND

a) Means within a column followed by the same letter are not significantly different at $p \leq 0.05$.
b) ND, not detected. Results are represented as mean±SD of duplicate tests.

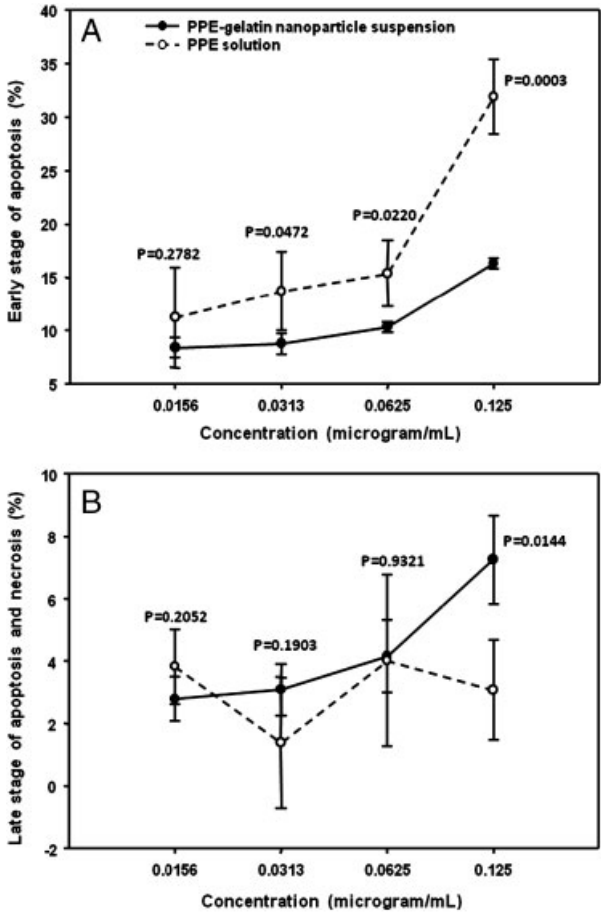

Figure 5. Percentage of early stage of apoptosis (A) and late stage of apoptosis and necrosis (B) of HL-60 cancer cells, treated by PPE-gelatin nanoparticle suspension fabricated using PPE-to-gelatin mass ratio 5:5, and PPE solution. Data are mean± SD of four replicates.

In the present study, only punicalagin was able to bind gelatin to form nanoparticles. Tannins of smaller molecular weight, such as ellagic acid and ellagic acid-hexoside, lack tertiary structures and binding capacity [22]. On the contrary, punicalagin, with the higher molecular weight (MW 1084), has a larger and more complex molecular structure providing sufficient affinity toward gelatin to form nanoparticles. Conformation of tannin molecules also affects affinity for gelatin. It has been reported that ellagitannin, compared to gallotannins, had intramolecular biphenyl linkages that can constrain aromatic rings in hydroxydiphenoyl groups, leading to the loss of conformational freedom [20]. Such structural characteristics enhance binding between ellagitannin and gelatin; however, they may negatively impact affinity for other proteins, such as bovine serum albumin [20]. In our study, both punicalagin anomers were bound with gelatin to form nanoparticles; however, punicalagin A showed higher loading efficiency than punicalagin B, suggesting higher affinity between punicalagin A and gelatin (Table 2).

FTIR spectra of PPE-gelatin nanoparticle showed that peaks at 1665 and 1535 cm^{-1} were shifted toward lower wavenumbers from correspondent peaks in gelatin and PPE. The intensity of peaks at 1699 and 1558 cm^{-1} in gelatin FTIR spectra was lower than those in PPE-gelatin nanoparticle FTIR spectra, suggesting that carbonyl C = O stretching vibration in pomegranate ellagitannins was involved in PPE-gelatin nanoparticles. The major binding force appeared to be hydrogen bonding, which was consistent with the appearances of peaks at 1665 and 1535 cm^{-1}, and with the disappearance of hydroxyl groups (peak in the range of 3500–3600 cm^{-1}) in gelatin FTIR spectra [13, 14, 18, 23].

Formation of PPE-gelatin nanoparticles is also influenced by PPE-to-gelatin mass ratio [24, 25]. When a small amount of tannins are added into a gelatin solution, tannin molecules deposit onto gelatin molecules via hydrogen binding and hydrophobic interactions. As the tannin content increases, single gelatin molecules adsorb more tannin molecules, which cause an increase in particle size. In this study, the particle size with PPE-to-gelatin mass ratios of 1:5, 5:5, and 7:5 were 101.9±9.0, 149.3±1.8, and 228.5±4.9 nm, respectively. The particle sizes measured by DLS appeared bigger than those in SEM photograph (Fig. 3). This was because lyophilized dry particles were used in SEM analysis [26]. Stability of the nanoparticle system in suspension is impacted by zeta-potential

of nanoparticles [27, 28]. Nanoparticles with higher zeta-potentials are more stable in solution due to static repulsion of particles. In this study, zeta-potentials of the nanoparticle suspensions were around +18 mV. The resultant nanoparticles under these three mass ratios were stable opalescent suspensions in deionized water.

Uptake of nanoparticles in vivo depends on particle size, zeta-potential, and morphology of nanoparticles. In the gastrointestinal tract, nanoparticles are absorbed into epithelial cells by inter membranous diffusion and by endocytosis mediated by receptors on cell membranes [29, 30]. Nanoparticle endocytosis was thought to be the major route. Nanoparticles with a particle size below 500 nm were effectively absorbed by enterocytes in the gastrointestinal tract [29, 31, 32]. PPE-gelatin nanoparticles fabricated in this study had a favorable particle size for absorption. Nanoparticles with spherical morphology were found to be captured more easily by receptors on epithelial cells than particles of different shapes [33]. Surface charge (zeta-potential) of the nanoparticle is another factor that affects direct uptake [29, 30, 34]. It was reported that the mucin layer attached to the surface of epithelial cells has a negatively charged membrane. When positively charged nanoparticles approach the mucin layer, weak ionic interaction is established, prolonging the retention time between nanoparticles and epithelial cells and eventually enhancing the entrapment of nanoparticles in epithelial cells [30]. Nanoparticles in the present study had the positively charged surface (around +18 mV). Therefore, we anticipate that PPE-gelatin nanoparticles may increase the absorption of ellagitannin in vivo. This is of importance because only 3–6% of ellagitannins were found to be absorbed from pomegranate juice [5, 35].

Bioactivities of a component are often altered once it is embedded into nanoparticles [36]. Pomegranate ellagitannins were known to induce cell-cycle arrest and apoptosis of cancer cells [37]. Punicalagin A and B were known to activate caspase-3 pathway and cleave poly-(ADP-ribose) polymerases, resulting in DNA fragmentation in HL-60 cells and apoptosis [37, 38]. PPE-gelatin nanoparticles were less effective than PPE in inducing the early stage of apoptosis, whereas they had similar effects in inducing late stage apoptosis and necrosis. We speculated that cell uptakes of nanoparticles may be a major reason for the observed differences in apoptotic effects. Our data suggested that PPE-gelatin nanoparticles have lower toxicity than pomegranate ellagitannins.

In conclusion, the PPE obtained from pomegranate pericarp contained punicalagin anomers, ellagic acid-hexoside, and ellagic acid. Punicalagin anomers had the capacity of binding gelatin to form nanoparticles. The nanoparticle fabricated using three PPE-to-gelatin mass ratios had the particle size <250 nm, zeta-potential around +18 mV, spherical morphology, and good loading efficiency and loading capacity. PPE-gelatin nanoparticles had lower apoptotic effects in HL-60 cells compared to PPE solution.

This study was supported in part by 2010 Research Opportunity Fund of University of Florida. Part of the work in this paper was used to file a provisional patent. We sincerely acknowledge Paul Carpinone, Gary Scheiffele, and Cheryl Rowe for their technical assistance with the operation of SEM, FTIR, and cell culture.

The authors have declared no conflict of interest.

5 References

[1] Buzea, C., Pacheco, I. I., Robbie, K., Nanomaterials and nanoparticles: Sources and toxicity. *Biointerphases* 2007, *2*, MR17–MR71.

[2] Siddiqui, I. A., Adhami, V. M., Bharali, D. J., Hafeez, B. B. et al., Introducing nanochemopreention as a novel approach for cancer control: proof of principle with green tea polyphenol epigallocatechin-3-gallate. *Cancer Res.* 2009, *69*, 1712–1716.

[3] Parveen, S., Mitra, M., Krishnakumar, S., Sahoo, S. K., Enhanced antiproliferative activity of carboplatin-loaded chitosan-alginate nanoparticles in a retinoblastoma cell line. *Acta Biomater.* 2010, *6*, 3120–3131.

[4] Tseng, C.-L., Su, W.-Y., Yen, K.-C., Yang, K.-C., Lin, F.-H., The use of biotinylated-EGF-modified gelatin nanoparticle carrier to enhance cisplatin accumulation in cancerous lungs via inhalation. *Biomaterials* 2009, *30*, 3476–3485.

[5] Cerdá, B., Llorach, R., Cerón, J. J., Espín, J. C., Tomás-Barberán, F. A., Evaluation of the bioavailability and metabolism in the rat of punicalagin, an antioxidant polyphenol from pomegranate juice. *Eur. J. Nutr.* 2003, *42*, 18–28.

[6] Seeram, N., Lee, R., Hardy, M., Heber, D., Rapid large scale purification of ellagitannins from pomegranate husk, a by-product of the commercial juice industry. *Sep. Purif. Technol.* 2005, *41*, 49–55.

[7] Kaplan, M., Hayek, T., Raz, A., Coleman, R. et al., Pomegranate juice supplementation to atherosclerotic mice reduces macrophage lipid peroxidation, cellular cholesterol accumulation and development of atherosclerosis. *J. Nutr.* 2001, *131*, 2082–2089.

[8] Adams, L. S., Seeram, N. P., Aggarwal, B. B., Takada, Y. et al., Pomegranate juice, total pomegranate ellagitannins, and punicalagin suppress inflammatory cell signaling in colon cancer cells. *J. Agric. Food Chem.* 2006, *54*, 980–985.

[9] Heber, D., Seeram, N. P., Wyatt, H., Henning, S. M. et al., Safety and antioxidant activity of a pomegranate ellagitannin-enriched polyphenol dietary supplement in overweight individuals with increased waist size. *J. Agric. Food Chem.* 2007, *55*, 10050–10054.

[10] Seeram, N. P., Aronson, W. J., Zhang, Y., Henning, S. M. et al., Pomegranate ellagitannin-derived metabolites inhibit prostate cancer growth and localize to the mouse prostate gland. *J. Agric. Food Chem.* 2007, *55*, 7732–7737.

[11] Simon, C., Barathieu, K., Laguerre, M., Schmitter, J.-M. et al., Three-dimensional structure and dynamics of

wine tannin–saliva protein complexes. A multitechnique approach. *Biochemistry* 2003, *42*, 10385–10395.

[12] Gawel, R., Red wine astringency: a review. *Aust. J. Grape Wine Res.* 1998, *4*, 74–95.

[13] Mousia, Z., Farhat, I. A., Pearson, M., Chesters, M. A., Mitchell, J. R., FTIR microspectroscopy study of composition fluctuations in extruded amylopectin-gelatin blends. *Biopolymers* 2001, *62*, 208–218.

[14] Chang, M. C., Ko, C.-C., Douglas, W. H., Preparation of hydroxyapatite-gelatin nanocomposite. *Biomaterials* 2003, *24*, 2853–2862.

[15] Kulkarni, A. P., Aradhya, S. M., Divakar, S., Isolation and identification of a radical scavenging antioxidant - punicalagin from pith and carpellary membrane of pomegranate fruit. *Food Chem.* 2004, *87*, 551–557.

[16] Meghashri, S., Vijay Kumar, H., Gopal, S., Antioxidant properties of a novel flavonoid from leaves of Leucas aspera. *Food Chem.* 2010, *122*, 105–110.

[17] Payne, K. J., Veis, A., Fourier transform ir spectroscopy of collagen and gelatin solutions: Deconvolution of the amide I band for conformational studies. *Biopolymers* 1988, *27*, 1749–1760.

[18] Kuo, S. W., Chang, F. C., Studies of miscibility behavior and hydrogen bonding in blends of poly(vinylphenol) and poly (vinylpyrrolidone). *Macromolecules* 2001, *34*, 5224–5228.

[19] Hagerman, A. E., Butler, L. G., The specificity of proanthocyanidin-protein interactions. *J. Biol. Chem.* 1981, *256*, 4494–4497.

[20] Deaville, E. R., Green, R. J., Mueller-Harvey, I., Willoughby, I., Frazier, R. A., Hydrolyzable tannin structures influence relative globular and random coil protein binding strengths. *J. Agric. Food Chem.* 2007, *55*, 4554–4561.

[21] Haslam, E., Natural polyphenols (vegetable tannins) as drugs: possible modes of action. *J. Nat. Prod.* 1996, *59*, 205–215.

[22] Barch, D. H., Rundhaugen, L. M., Stoner, G. D., Pillay, N. S., Rosche, W. A., Structure-function relationships of the dietary anticarcinogen ellagic acid. *Carcinogenesis* 1996, *17*, 265–269.

[23] Rehman, I., Bonfield, W., Characterization of hydroxyapatite and carbonated apatite by photo acoustic FTIR spectroscopy. *J. Mater. Sci. Mater. Med.* 1997, *8*, 1–4.

[24] Yi, K., Cheng, G., Xing, F., Gelatin/tannin complex nanospheres via molecular assembly. *J. Appl. Polym. Sci.* 2006, *101*, 3125–3130.

[25] Kawamoto, H., Nakatsubo, F., Murakami, K., Stoichiometric studies of tannin-protein co-precipitation. *Phytochemistry* 1996, *41*, 1427–1431.

[26] Zhong, Q., Jin, M., Zein nanoparticles produced by liquid-liquid dispersion. *Food Hydrocolloids* 2009, *23*, 2380–2387.

[27] Jahanshahi, M., Babaei, Z., Protein nanoparticle: a unique system as drug delivery vehicles. *Afr. J. Biotechnol.* 2008, *7*, 4926–4934.

[28] Mohanraj, V. J., Chen, Y., Nanoparticles- a review. *Trop. J. Pharmac. Res.* 2006, *5*, 561–573.

[29] Acosta, E., Bioavailability of nanoparticles in nutrient and nutraceutical delivery. *Curr. Opin. Colloid Interface Sci.* 2009, *14*, 3–15.

[30] des Rieux, A., Fievez, V., Garinot, M., Schneider, Y.-J., Préat, V., Nanoparticles as potential oral delivery systems of proteins and vaccines: A mechanistic approach. *J. Control. Release* 2006, *116*, 1–27.

[31] Desai, M. P., Labhasetwar, V., Amidon, G. L., Levy, R. J., Gastrointestinal uptake of biodegradable microparticles: effect of particle size. *Pharm. Res.* 1996, *13*, 1838–1845.

[32] Jani, P., Halbert, G. W., Langridge, J., Florence, A. T., Nanoparticle uptake by the rat gastrointestinal mucosa: quantitation and particle size dependency. *J. Pharm. Pharmacol.* 1990, *42*, 821–826.

[33] Opanasopit, P., Apirakaramwong, A., Ngawhirunpat, T., Rojanarata, T., Ruktanonchai, U., Development and characterization of pectinate micro/nanoparticles for gene delivery. *AAPS PharmSciTech* 2008, *9*, 67–74.

[34] Takeuchi, H., Yamamoto, H., Kawashima, Y., Mucoadhesive nanoparticulate systems for peptide drug delivery. *Adv. Drug Deliv. Rev.* 2001, *47*, 39–54.

[35] Cerda, B., Ceron, J. J., Tomas-Barberan, F. A., Espin, J. C., Repeated oral administration of high doses of the pomegranate ellagitannin punicalagin to rats for 37 days is not toxic. *J. Agric. Food Chem.* 2003, *51*, 3493–3501.

[36] Powers, K. W., Brown, S. C., Krishna, V. B., Wasdo, S. C. et al., Research strategies for safety evaluation of nanomaterials. Part VI. Characterization of nanoscale particles for toxicological evaluation. *Toxicol. Sci.* 2006, *90*, 296–303.

[37] Chen, L.-G., Huang, W.-T., Lee, L.-T., Wang, C.-C., Ellagitannins from Terminalia calamansanai induced apoptosis in HL-60 cells. *Toxicol. In Vitro* 2009, *23*, 603–609.

[38] Surh, Y.-J., Molecular mechanisms of chemopreventive effects of selected dietary and medicinal phenolic substances. *Mutat. Res.* 1999, *428*, 305–327.

